
7

Characterization of Acetylcholine Release and the Compensatory Contribution of Non-Ca_v2.1 Channels at Motor Nerve Terminals of *Leaner* Ca_v2.1-Mutant Mice

Simon Kaja,^{1,2#} Rob C.G. Van de Ven,^{3#} Ludo A.M. Broos,³ Rune R. Frants,³
Michel D. Ferrari,¹ Arn M.J.M. van den Maagdenberg,^{1,3} and Jaap J. Plomp^{1,2}

*Department of ¹Neurology, ²Molecular Cell Biology - Group Neurophysiology and
³Human Genetics, Leiden University Medical Centre, Leiden, The Netherlands;*

#These authors contributed equally to this work.

Neuroscience, in press

Abstract

The severely ataxic and epileptic mouse *leaner* (*Ln*) carries a natural splice site mutation in *Cacna1a*, leading to a C-terminal truncation of the encoded $\text{Ca}_v2.1 \alpha_1$ protein. $\text{Ca}_v2.1$ is a neuronal Ca^{2+} channel, mediating neurotransmitter release at many central synapses and the peripheral neuromuscular junction (NMJ). With electrophysiological analyses we demonstrate severely reduced (~50%) neurotransmitter release at *Ln* NMJs. This equals the reduction at NMJs of *Cacna1a* null-mutant ($\text{Ca}_v2.1$ -KO) mice, which display a neurological phenotype remarkably similar to that of *Ln* mice. However, using selective Ca_v channel blocking compounds we revealed a compensatory contribution profile of non- $\text{Ca}_v2.1$ type channels at *Ln* NMJs that differs completely from that at $\text{Ca}_v2.1$ -KO NMJs. Our data indicate that the residual function and presence of *Ln*-mutated $\text{Ca}_v2.1$ channels precludes presynaptic compensatory recruitment of Ca_v1 and $\text{Ca}_v2.2$ channels, and hampers that of $\text{Ca}_v2.3$ channels. This is the first report directly showing at single synapses the deficits and plasticity in transmitter release resulting from the *Ln* mutation of *Cacna1a*.

A small part of the present results has been presented in preliminary form at the Xth International Conference on Myasthenia Gravis and Related Disorders (2002, Key Biscayne, USA), and has been published in short in the conference proceedings (Plomp et al., 2003).

Acknowledgements

We thank Dr. J.N. Noordermeer (Dept. of Molecular Cell Biology) for use of the fluorescence microscope and M.G.M. Deenen and H. Choufoer (Dept. of Neurosurgery) for help with muscle fibre histology. This work was supported by grants from the Prinses Beatrix Fonds (#MAR01-0105, to JJP), the Hersenstichting Nederland (#9F01(2).24, to JJP), KNAW van Leersumfonds (to JJP), the Netherlands Organisation for Scientific Research, NWO (an EMBL travel bursary to SK, and a VICI grant 918.56.602, to MDF), a 6th Framework specific targeted research project EUROHEAD (LSHM-CT-2004-504837, to MDF) and the Centre for Medical Systems Biology (CMSB) established by the Netherlands Genomics Initiative/Netherlands Organisation for Scientific Research (NGI/NWO).

Introduction

Pore-forming subunits of neuronal voltage-activated Ca²⁺ channels are a family of membrane proteins encoded by different genes that are expressed widely throughout the nervous system (Catterall, 2000). The channel subtypes Ca_v2.1 (P/Q-type), Ca_v2.2 (N-type) and Ca_v2.3 (R-type) are mainly involved in mediating neurotransmitter release from central and peripheral nerve terminals. Their specialized synaptic function most likely results from their ability to localize at active zones (the presynaptic transmitter release sites), and to interact with neuroexocytotic proteins (Spafford and Zamponi, 2003; Jones, 2003).

Studies in mice and rats have shown that joint contribution of Ca_v2.1, -2 and -3 channel subtypes to transmitter release is common during early development at synapses of several CNS areas (cerebral cortex, cerebellum, thalamus, hippocampus, spinal cord) (Iwasaki et al., 2000; Kamp et al., 2005). However, during the first few postnatal weeks, the contribution of Ca_v2.2 and Ca_v2.3 is gradually lost and taken over by Ca_v2.1 channels at many types of synapses (Iwasaki et al., 2000). At only a small subset (e.g. in cerebral cortex and hippocampus) release remains jointly mediated by Ca_v2.1, -2 and -3 channels (Luebke et al., 1993; Wheeler et al., 1994; Iwasaki et al., 2000). At the peripheral neuromuscular junction (NMJ), studies in rodents showed a similar developmental switch, gradually eliminating Ca_v2.2 contribution (Urbano et al., 2002), leaving Ca_v2.1 channels to control the main part (>90%) of nerve action potential-evoked release of acetylcholine (ACh) from a few weeks postnatally and onwards (Uchitel et al., 1992; Bowersox et al., 1995; Hong and Chang, 1995; Lin and Lin-Shiau, 1997).

Interestingly, the capability of joint contribution of Ca_v2.1, -2, and -3 channels to transmitter release is not permanently lost after the developmental switch, but seems to be rather generally preserved as a compensatory mechanism in case of malfunction of the original, monospecifically contributing channel. Thus, NMJs and central synapses of Ca_v2.1 *null*- and missense-mutant mice become to rely on Ca_v1, Ca_v2.2 and/or Ca_v2.3 channels (Qian and Noebels, 2000; Leenders et al., 2002; Urbano et al., 2003; Pagani et al., 2004; Cao et al., 2004; Inchauspe et al., 2004; Ishikawa et al., 2005; Etheredge et al., 2005; Kaja et al., 2006), whereas compensatory Ca_v2.1 expression occurs in Ca_v2.2 *null*-mutant neurons (Takahashi et al., 2004b). Cultured cerebellar Purkinje cells are able of upregulating Ca_v2.3 channels after partial downregulation of Ca_v2.1 channels by antibodies (Pinto et al., 1998).

Ca_v2.1 channels have been implicated in human neurological disease. Mutations in *CACNA1A*, the coding gene for the α_1 -subunit, were identified in familial hemiplegic migraine type-1, episodic ataxia type-2 (EA2), spinocerebellar ataxia type-6 and generalised epilepsy with ataxia (Ophoff et al., 1996; Zhuchenko et al., 1997; Jouvenceau et al., 2001; Imbrici et al., 2004). Furthermore, Ca_v2.1 channels at the NMJ are auto-immune targets in the neuro-immunological Lambert-Eaton myasthenic syndrome (Lennon et al., 1995). Compensatory expression of non-Ca_v2.1 channels may help reduce symptoms in these diseases.

A number of natural and transgenic *Cacnala* mouse mutants, displaying a spectrum of symptoms of epilepsy and ataxia, serve as models of human Ca_v2.1 channelopathies. These include the natural mutants *leaner* (*Ln*), *tottering* and *rolling Nagoya* (Fletcher et al., 1996; Doyle et al., 1997; Lorenzon et al., 1998; Mori et al., 2000), knock-outs (Jun et al., 1999; Fletcher et al., 2001) and knock-ins (Van Den Maagdenberg et al., 2004; Kaja et al., 2004). Characterization of the primary neuronal deficits and subsequent compensatory involvement of non-Ca_v2.1 channels in these mouse models is of particular interest. The underlying signalling pathways may harbour drug targets that might be influenced to optimize compensation.

In the present study we characterized the basic aspects of transmitter release and the compensatory contribution of non-Ca_v2.1 channels at the NMJ of natural *Ln* mutant mice. The *Ln*-Ca_v2.1 α_1 protein lacks a large part of the cytoplasmic C-terminus (Fletcher et al., 1996; Doyle et al., 1997), which contains important sites for interaction with other structural and functional synaptic proteins (Catterall, 1999; Lee et al., 1999; Maximov et al., 1999). Previously, we have shown that the mouse NMJ is a suitable model to study the synaptic effect of *CACNA1A* mutations on transmitter release (Plomp et al., 2000; Van Den Maagdenberg et al., 2004; Kaja et al., 2005). With electrophysiological measurements and selective Ca_v channel blocking compounds we here compared the ACh release characteristics of *Ln* NMJs with that of Ca_v2.1 knock-out mice (Ca_v2.1-KO), in which Ca_v2.1 channels are absent but compensated for by Ca_v2.2 and -3 channels (Urbano et al., 2003; Pagani et al., 2004). In spite of a remarkably similar neurological phenotype of these two mice strains, i.e. severe and progressive ataxia and epilepsy leading to premature death at about 3-4 weeks of age (Yoon, 1969; Jun et al., 1999), we found only limited Ca_v2.3 channel contribution at *Ln* NMJs, and no Ca_v2.2 channel contribution at all. Our data indicate that the presence of truncated *Ln*-Ca_v2.1 α_1 protein blocks compensatory contribution of Ca_v2.2 channels and greatly inhibits that of Ca_v2.3 channels at the NMJ.

Materials and Methods

Mice

All animal experiments were in accordance with national legislation, the USA National Institutes of Health recommendations for the humane use of animals, and were approved by the Leiden University Animal Experiments Committee.

We generated Ca_v2.1-KO mice, essentially as described by others (Jun et al., 1999). Briefly, mouse genomic DNA clones were derived from a pPAC4 library (129/SvevTACfBr strain). In the targeting vector, an *MscI*-*XbaI* fragment that includes part of exon 4 and intron 4 was replaced by a PGK-driven *neo* cassette, thereby disrupting the *Cacna1a* gene. ES cells (E14) were electroporated and positive clones selected for homologous recombination by Southern blot analysis, using external probes. Correctly targeted ES cells were injected into blastocysts to create chimeric animals. F1 agouti progeny were genotyped for transmission of the mutant allele and further bred with C57Bl6J mice in order to create the transgenic Ca_v2.1-KO mouse line. Homozygous Ca_v2.1-KO mice of generation F3 were used for experiments. Successful targeting of the *Cacna1a* gene was shown by using standard molecular biological techniques similar to Jun et al. (Jun et al., 1999) (data not shown). The homozygous Ca_v2.1-KO mice exhibited a phenotype similar to that described by others (Jun et al., 1999; Fletcher et al., 2001), i.e. severe ataxia, epileptic seizures and premature death at 3-4 weeks of age.

Homozygous *Ln* mice were obtained from heterozygous breedings. Original breeders were purchased from Jackson Laboratories (Bar Harbor, ME, USA). Wild-types served as controls (littermates if possible, otherwise age-matched non-littermates). Mice were used for experiments at age P19-21. *Ln* and Ca_v2.1-KO mice body weights were ~55% lower than wild-type (4.5 ± 0.1 , 4.5 ± 0.2 and 10.2 ± 0.6 g, respectively, $n=11-16$, $p<0.001$).

Genotyping

Genomic DNA was extracted from tail clips. Tissue was incubated in 250 μ l incubation mixture (50 mM Tris-HCl pH 9.0, 0.45% Igepal [Sigma-Aldrich], 0.4 mg/ml Prot K) at 55 °C for 4 h. After heat inactivation (10 min, 95 °C), 0.2 μ l lysate was amplified by PCR.

For genotyping of Ca_v2.1-KO mice two PCR reactions were performed. Forward primer P277 5'-CTGAGCTGATGCTGAAGCTG-3', and reverse primer P279 5'-AGACTCAC-GCACTTGGGATT-3' were used for detection of the wild-type allele. For the second PCR detecting the mutant allele, forward primer P354 5'-TCGGGAGCGGCATACCGTAAAG-3', and reverse primer P355 5'-TCCGGCCGCTTGGGTGGAGA-3' were used, both located in the *neo* cassette. PCR products of 717 bp and 204 bp, respectively, were produced.

For genotyping of *Ln* mice, forward primer P204 5'-TCGACATGCCTAACAGCCAG-3' located on exon 42, and reverse primer P205 5'-CAGTACCCATTTCTCGCATC-3' located on exon 43, produced a fragment of 151 bp. Digestion of the wild-type fragment with *Mva*I resulted in two fragments of 121 bp and 30 bp, whereas the *Ln* fragment remained uncut.

Ex vivo neuromuscular junction electrophysiology

Mice were euthanized by carbon dioxide inhalation. Phrenic nerve-hemidiaphragms were dissected and mounted in standard Ringer's medium (in mM: NaCl 116, KCl 4.5, CaCl₂ 2, MgSO₄ 1, NaH₂PO₄ 1, NaHCO₃ 23, glucose 11, pH 7.4), at room temperature (20-22 °C) and continuously bubbled with 95% O₂ / 5% CO₂. Intracellular recordings of miniature endplate potentials (MEPPs, the postsynaptic depolarizing events due to spontaneous unquantal ACh release) and endplate potentials (EPPs, the depolarization resulting from nerve action potential-evoked ACh release) were made at NMJs at 28 °C using a 10-20 MΩ glass microelectrode, filled with 3 M KCl, connected to a Geneclamp 500B (Axon Instruments/Molecular Devices, Union City, CA, USA) for amplifying and filtering (10 kHz low-pass). Signals were digitized, stored and analyzed (off-line) on a personal computer using a Digidata 1322A interface, Clampex 8.2 and Clampfit 8.2 programs (all from Axon Instruments/Molecular Devices) and routines programmed in Matlab (The MathWorks Inc., Natick, MA, USA). At least 30 MEPPs and EPPs were recorded at each NMJ, and 7-15 NMJs were sampled per experimental condition per muscle. Muscle action potentials were blocked by 3 μM of the selective muscle Na⁺ channel blocker μ-conotoxin GIIIB (Scientific Marketing Associates, Barnet, Herts, UK). In order to record EPPs, the phrenic nerve was stimulated supramaximally at 0.3 Hz and 40 Hz, using either a bipolar platinum or a suction electrode. The amplitudes of EPPs and MEPPs were normalized to -75 mV, assuming 0 mV as the reversal potential for ACh-induced current (Magleby and Stevens, 1972). The normalized EPP amplitudes were corrected for non-linear summation according to (McLachlan and Martin, 1981) with an *f* value of 0.8. Quantal content, i.e. the number of ACh quanta released per nerve impulse, was calculated for each NMJ by dividing the normalized and corrected mean EPP amplitude by the normalized mean MEPP amplitude.

In order to assess the contribution of different Ca²⁺ current types on ACh release, EPPs and MEPPs were also measured in the presence of the specific Ca_v channel blockers ω-agatoxin-IVA (Ca_v2.1, 200 nM), ω-conotoxin-GVIA (Ca_v2.2, 2.5 μM), SNX-482 (Ca_v2.3, 1 μM) and nifedipine (Ca_v1, 10 μM, kept in the dark prior to the experiment). Measurements were made following a 20 min pre-incubation with toxin. All toxins were from Scientific Marketing Associates, Barnet, Herts, UK. Nifedipine (Sigma-Aldrich, Zwijndrecht, The Netherlands) was dissolved in dimethylsulfoxide to obtain a 10 mM stock solution. The final solution in Ringer's medium contained 0.1% dimethylsulfoxide. In the control condition before nifedipine incubation, electrophysiological measurements were made in Ringer's medium with 0.1% dimethylsulfoxide added. Nifedipine was pre-incubated for 1 h before starting the measurements. During pre-incubations and the electrophysiological measurements, 95% O₂ / 5% CO₂ was blown over the surface of the 2 ml medium.

α -Bungarotoxin staining and image analysis

NMJ size was determined by staining the area of ACh receptors with fluorescently labelled α -bungarotoxin (BTx), as described before (Kaja et al., 2005).

Muscle fibre diameter analysis

Midline muscle sections were excised from left hemidiaphragms, pinned out on blocks of silicone rubber, snap frozen in liquid nitrogen and subsequently embedded in TissueTek[®] (Bayer BV, Mijdrecht, The Netherlands). Transversal sections (12-18 μ m) were cut on a Microm cryostat (Adamas Instruments BV, Leersum, The Netherlands), at -21° C and collected on poly-lysine coated slides, dried for 1 h at room temperature, fixed for 10 s in ice-cold acetone, stained for 10 s in 0.5% alkaline toluidine blue, dehydrated in a graded series of ethanol (50%, 70%, 80%, 90%, 96%, 100%, 1 min each) and finally cleared with xylene. Sections were embedded in Entellan mounting medium (Merck, Darmstadt, Germany) and viewed under a Zeiss Axioplan light microscope (Zeiss, Jena, Germany). Digital photos were taken and fibre diameter quantified using ImageJ (National Institutes of Health, USA). Stereological considerations were taken into account by defining the actual diameter of a muscle fibre by the shortest distance measured. Ten to 15 fibres were measured per muscle.

Statistical analyses

Possible statistical differences were analysed with paired or unpaired Student's *t*-tests or analysis of variance (ANOVA) with Tukey's HSD post-hoc test, where appropriate, on grand group mean values (with *n* as the number of mice tested), calculated from the mean muscle values. Mean muscle values were calculated from the mean parameter values obtained at 6-15 NMJs per experimental condition. $P < 0.05$ was considered to be significant. The data are presented as mean \pm S.E.M.

Results

*Similar reduction of ACh release at NMJs of *Ln* and *Ca_v2.1-KO* mice*

We first studied the basic NMJ electrophysiology of *Ln* and our newly generated *Ca_v2.1-KO* mice. Spontaneous unquantal ACh release from motor nerve terminals, measured as MEPP frequency, was decreased by $\sim 50\%$ in both *Ln* and *Ca_v2.1-KO* mice, compared with wild-type (0.41 ± 0.04 and 0.34 ± 0.04 vs. 0.86 ± 0.06 s⁻¹, respectively, $n=13-18$ mice, $p < 0.001$; Figure 1A). MEPP amplitude, i.e. the size of the postsynaptic response to unquantal ACh release, was $\sim 20\%$ higher at both *Ln* and *Ca_v2.1-KO* NMJs ($n=13-18$, $p < 0.001$, Figures 1B, C).

Nerve stimulation-evoked ACh release upon low-rate (0.3 Hz) stimulation of the phrenic nerve was greatly reduced at both *Ln* and *Ca_v2.1-KO* NMJs, as judged from the EPP amplitudes that were only $\sim 65\%$ of wild-type ($n=13-18$ mice, $p < 0.001$, Figures 1D, E). The quantal contents, calculated from EPP and MEPP amplitudes, were $\sim 50\%$ reduced (31.2 ± 1.1 , 16.4 ± 1.2 and 13.9 ± 0.5 at wild-type, *Ln* and *Ca_v2.1-KO* NMJs, respectively, $n=13-18$ mice, $p < 0.001$, Figure 1F).

We also studied the short-term depression of ACh release during high-rate (40 Hz) nerve stimulation, which approximates the physiological firing rate of rodent motor nerves (Eken, 1998). Both *Ln* and *Ca_v2.1-KO* showed a significantly more pronounced rundown of EPP amplitudes than that seen in wild-type (Figures 2A, B). The average amplitude of the 21st-35th EPP (e.g. the plateau phase) of the trains, expressed as percentage of the amplitude of the first EPP, was 68 ± 1 , 65 ± 2 and $77 \pm 1\%$ at *Ln*, *Ca_v2.1-KO* and wild-type NMJs, respectively ($n=6$ mice, $p < 0.001$, Figure 2C). During the plateau phase, EPP amplitudes at *Ln* and *Ca_v2.1-KO* NMJs fluctuated much more than at wild-types. The coefficient of variance

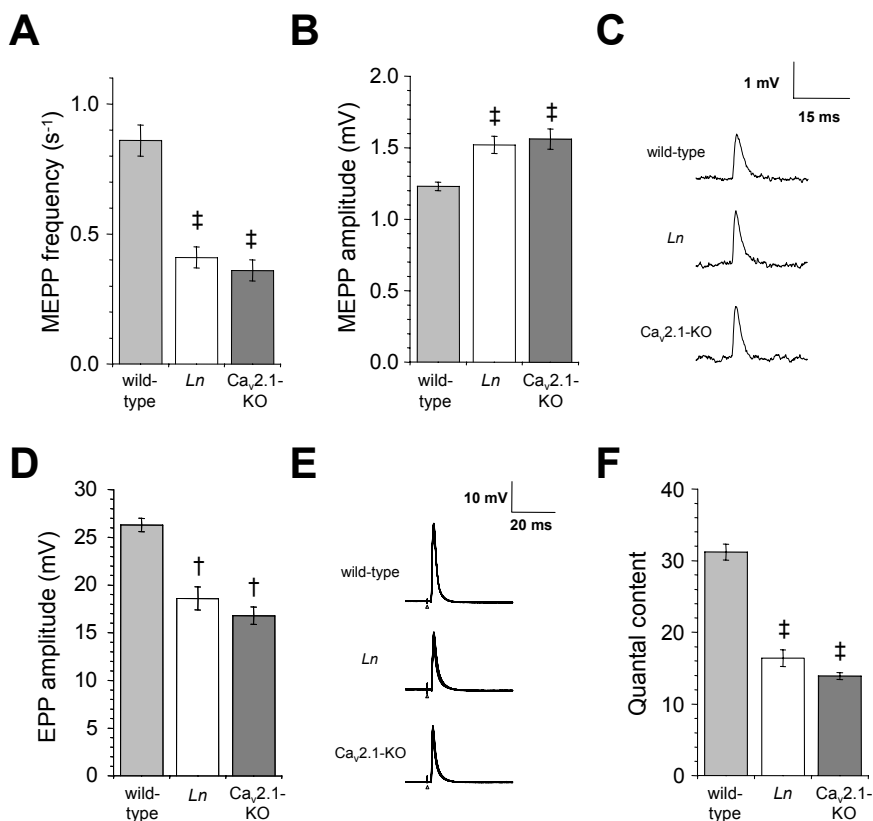


Figure 1. ACh release is reduced at the *Ln* NMJ, compared to wild-type. The extent of reduction is similar to that found at $Ca_v2.1$ -KO NMJs.

(A) Spontaneous unquantal ACh release, measured as MEPP frequency. (B) MEPP amplitude was ~25% increased at *Ln* and $Ca_v2.1$ -KO NMJs. (C) Example MEPP recordings. (D) Low-rate (0.3 Hz) evoked EPP amplitude is ~35% reduced at *Ln* and $Ca_v2.1$ -KO NMJs, compared to wild-type. (E) Example 0.3 Hz EPP recordings. For each genotype, 20 superimposed EPPs are shown. Triangles indicate moment of nerve stimulation. (F) The calculated quantal content was reduced by about half at both *Ln* and $Ca_v2.1$ -KO NMJs. †p<0.01, ‡p<0.001, different from wild-type.

of the 21st-35th EPP amplitude was 0.06 ± 0.01 , 0.19 ± 0.02 and 0.25 ± 0.02 at wild-type, *Ln* and $Ca_v2.1$ -KO NMJs, respectively (n=6 mice, p<0.001, Figure 2D).

*Compensatory contribution of non- $Ca_v2.1$ channels at *Ln* and $Ca_v2.1$ -KO NMJs*

In wild-type mice, nerve stimulation-evoked neurotransmitter release at the NMJ is dependent almost exclusively on $Ca_v2.1$ channels (Uchitel et al., 1992; Bowersox et al., 1995; Giovannini et al., 2002; Van Den Maagdenberg et al., 2004). It has been reported that the $Ca_v2.1$ deficiency at NMJs of $Ca_v2.1$ -KO mice is compensated for by $Ca_v2.2$ and -3 channels (Urbano et al., 2003). Here we studied such compensatory contribution of non- $Ca_v2.1$ channels at *Ln* NMJs, using selective Ca_v blocking compounds, and compared it with NMJs of the $Ca_v2.1$ -KO mice generated in our laboratory and wild-type mice.

At wild-type NMJs, ω -agatoxin-IVA (200 nM) reduced 0.3 Hz nerve stimulation-evoked ACh release by $96.2 \pm 0.7\%$ (quantal content before and after application of toxin was 31.3 ± 1.6 and 1.2 ± 0.2 , n=4 mice, p<0.001, Figure 3A), confirming the almost complete dependence on $Ca_v2.1$ channels. The quantal content at wild-type NMJs did not change upon incubation with either ω -conotoxin-GVIA (2.5 μ M), SNX-482 (1 μ M) or nifedipine (10 μ M),

indicating that $\text{Ca}_v2.2$, $\text{Ca}_v2.3$ and Ca_v1 channels do not contribute to ACh release at the wild-type NMJ.

At NMJs of $\text{Ca}_v2.1$ -KO mice, as expected, evoked ACh release was ω -agatoxin-IVA-insensitive, confirming the absence of $\text{Ca}_v2.1$ channels (Figure 3). The quantal content was 14.5 ± 0.3 and 14.0 ± 0.5 before and after application of the toxin, respectively ($n=3$ mice, $p=0.21$). However, $\text{Ca}_v2.2$ blocker ω -conotoxin-GVIA reduced the quantal content by $22.1 \pm 6.3\%$ (13.3 ± 1.2 and 10.2 ± 0.9 before and after application of toxin, respectively, $n=6$ mice, $p<0.05$, Figure 3). The $\text{Ca}_v2.3$ blocker SNX-482 reduced the quantal content (by $\sim 50\%$, from 15.2 ± 0.7 to 7.6 ± 2.0 , $n=4$, $p<0.05$, Figure 3), as did the Ca_v1 channel blocker nifedipine (by $\sim 27\%$, from 13.5 ± 0.7 to 9.8 ± 0.8 , $n=4$ mice, $p<0.01$, Figure 3). These results show that there is joint contribution of Ca_v1 , $\text{Ca}_v2.2$ and $\text{Ca}_v2.3$ channels in evoked ACh release, compensating for the deficiency of $\text{Ca}_v2.1$ channels at $\text{Ca}_v2.1$ -KO NMJs.

At the *Ln* NMJ, however, a very different picture emerged. ω -Agatoxin-IVA reduced the evoked ACh release by $\sim 60\%$ (quantal content decreased from 15.9 ± 1.2 to 6.1 ± 0.4 , $n=4$ mice, $p<0.001$, Figure 3). A small proportion ($\sim 13\%$) of evoked ACh release at *Ln* NMJs was SNX-482 sensitive (the quantal content decreased from 15.7 ± 1.1 to 13.7 ± 0.7 , $n=6$ mice, $p<0.05$, Figure 3). ω -Conotoxin-GVIA or nifedipine did not change quantal content (Figure 3).

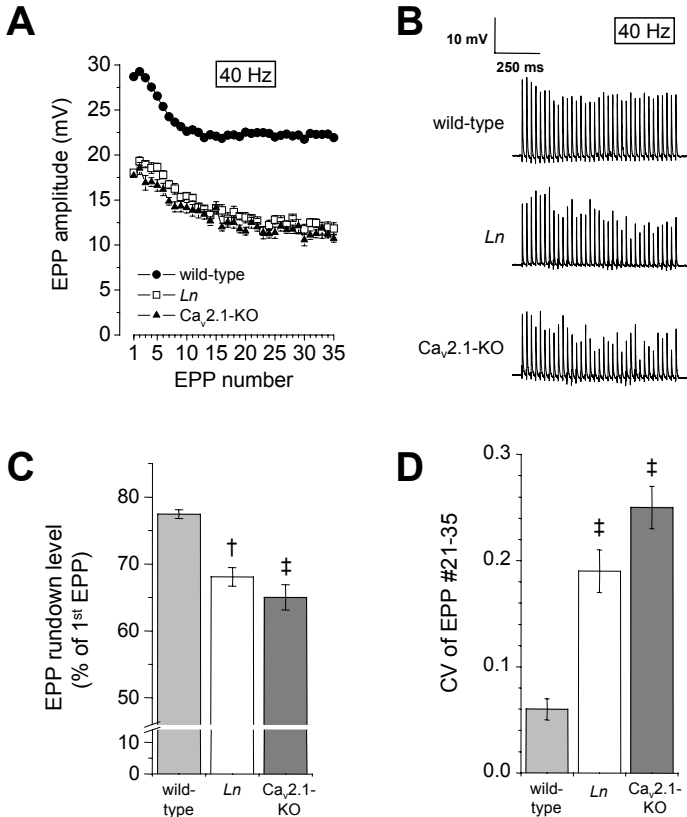


Figure 2. Increased rundown of EPP amplitude during high-rate (40 Hz) nerve stimulation at both *Ln* and $\text{Ca}_v2.1$ -KO NMJs. (A) Averaged EPP amplitude rundown profiles. (B) Representative 1 s recording traces of 40 Hz EPP trains. (C) Normalized EPP amplitude rundown level (mean EPP amplitude of the 21st-35th EPP, expressed as percentage of the first EPP) is more pronounced at both *Ln* and $\text{Ca}_v2.1$ -KO NMJs. (D) *Ln* and $\text{Ca}_v2.1$ -KO NMJs display larger coefficient of variance (CV), compared to wild-type, of the amplitude of EPP number 21-35 of a 40 Hz train. [†] $p<0.01$, [‡] $p<0.001$, different from wild-type.

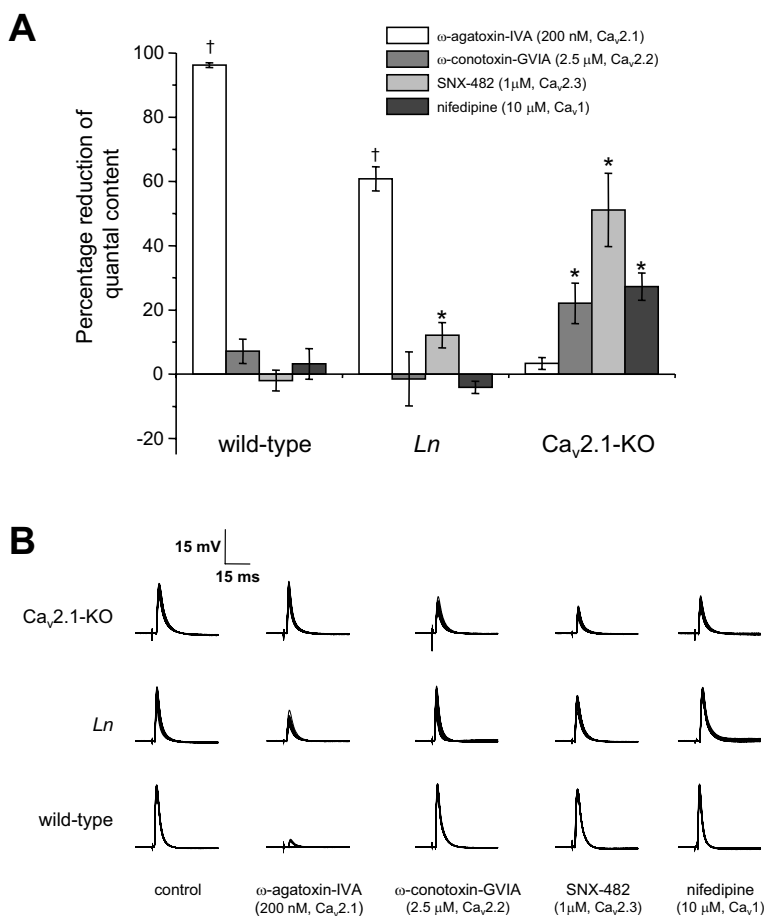


Figure 3. Differential effects of blockers of specific Ca_v channels on 0.3 Hz evoked ACh release at the wild-type, *Ln* and $Ca_v2.1$ -KO NMJ.

(A) Effect on quantal content. Values represent the mean percentage of reduction of quantal content induced by the specific compound. N=3-7 mice per condition, 6-15 NMJs measured per muscle. * $p < 0.05$, [†] $p < 0.01$, different from control the condition before application of the blocking compound. (B) Representative EPP recording traces. Ten superimposed EPPs are drawn per condition and genotype.

These data show compensatory contribution of $Ca_v2.3$ channels at *Ln* NMJs and, furthermore, that ~25% of the evoked ACh release is not blocked by the compounds used, suggesting compensatory contribution of another, unknown Ca_v channel. It might be speculated that the *Ln* mutation renders the $Ca_v2.1$ channel less sensitive to ω -agatoxin-IVA and that 200 nM of the toxin is a sub-optimal concentration that only blocks part of the $Ca_v2.1$ channels. Therefore, we tested the effect of 600 nM of the toxin in one *Ln* muscle. The quantal content decreased by ~67% (from 16.1 ± 0.9 to 5.3 ± 0.5 , 10 NMJs sampled before and during toxin incubation, $p < 0.001$). This reduction is similar to that induced by 200 nM ω -agatoxin-IVA, indicating that *Ln*- $Ca_v2.1$ channels retain normal ω -agatoxin-IVA sensitivity.

Spontaneous unquantal ACh release at wild-type NMJs, measured as MEPP frequency, was reduced by 200 nM ω -agatoxin-IVA, as published before by us and others (Plomp et al., 2000; Giovannini et al., 2002; Van Den Maagdenberg et al., 2004; Kaja et al., 2005), by 72.4 \pm 2.2%, from 0.95 ± 0.07 to 0.26 ± 0.01 , n=4 mice ($p < 0.01$). All other Ca_v blockers tested

had no effect on wild-type MEPP frequency (Table 1). At Ca_v2.1-KO NMJs, only SNX-482 (1 μM) reduced MEPP frequency, by 39.1 ± 8.7%, from 0.42 ± 0.07 to 0.25 ± 0.05 s⁻¹ (n=4 mice, p<0.05, Table 1), while all other blockers did not change this parameter. At *Ln* NMJs, ω-agatoxin-IVA, but not the other blockers, reduced MEPP frequency by ~30% (from 0.53 ± 0.05 to 0.38 ± 0.06, n=4 mice, p<0.05, Table 1). Thus, *Ln*-Ca_v2.1 channels still contribute to some extent to spontaneous ACh release and there is no compensatory contribution by Ca_v2.2, Ca_v2.3 or Ca_v1 channels. The abolished Ca_v2.1 contribution at Ca_v2.1-KO NMJs is partly compensated for by Ca_v2.3 channels.

Table 1. Effect of specific Ca_v blockers on spontaneous uniquantal ACh release.

Compound - (selectivity)	wild-type	<i>Ln</i>	Ca _v 2.1-KO
ω-agatoxin-IVA - (Ca _v 2.1)	72.4 ± 2.2%†	27.0 ± 8.0%*	-3.5 ± 13.4%
ω-conotoxin-GVIA - (Ca _v 2.2)	7.0 ± 7.6%	-11.3 ± 19.8%	-8.6 ± 3.4%
SNX-482 - (Ca _v 2.3)	-2.4 ± 5.2%	9.1 ± 7.2%	39.1 ± 8.7%*
nifedipine - (Ca _v 1)	-13.1 ± 11.7%	8.0 ± 13.5%	12.4 ± 16.2%

Comparison of the effect of various blockers of Ca_v channels on spontaneous ACh release, measured as MEPP frequency, at wild-type, *Ln* and Ca_v2.1-KO NMJs. Data is expressed as the percentage change induced by the compound of the mean MEPP frequency measured in the control period before compound application. N=3-6 mice per condition, 6-15 NMJs measured per muscle.

*p<0.05, †p<0.01, different from the condition before application of the blocking compound.

*Reduction of NMJ size and muscle fibre diameter at both *Ln* and Ca_v2.1-KO mice*

ACh release at the NMJ is roughly correlated with NMJ size (Kuno et al., 1971; Harris and Ribchester, 1979), and reduced NMJ size has indeed been reported for Ca_v2.1-KO mice (Urbano et al., 2003). In view of this, the observed reduced ACh release at NMJs of *Ln* mice may be associated with a NMJ size reduction as well. We quantified the size of postsynaptic ACh receptor clusters as identified by Alexa Fluor 488 conjugated BTx. The area, width and perimeter of the stained surface at *Ln* NMJs was reduced by 11-26%, compared to wild-type (n=5 mice, 15 NMJs per muscle, Table 2). Ca_v2.1-KO NMJs showed similar reductions (Table 2). We also quantified muscle fibre diameter. Measurement of toluidine blue stained transversal freeze sections revealed ~45% reduced fibre diameter, compared to wild-type, in both *Ln* and Ca_v2.1-KO diaphragms (n=3 mice, 15 fibres per muscle, p<0.01, Table 2).

Table 2. Reduced NMJ size and muscle fibre diameter in *Ln* and Ca_v2.1-KO diaphragm.

Size parameter	wild-type	<i>Ln</i>	Ca _v 2.1-KO
NMJ area (μm ²)	328.7 ± 11.5	243.0 ± 13.6† (-26%)	212.2 ± 18.3‡ (-35%)
NMJ perimeter (μm)	74.4 ± 2.4	66.3 ± 2.1* (-11%)	64.1 ± 0.7† (-14%)
NMJ length (μm)	28.3 ± 1.4	27.0 ± 0.8	25.7 ± 0.6
NMJ width (μm)	14.4 ± 0.4	12.5 ± 0.4* (-13%)	11.8 ± 0.4† (-18%)
Fibre diameter (μm)	18.1 ± 2.3	10.9 ± 0.9* (-40%)	8.7 ± 0.9* (-52%)

Quantification of NMJ size (fluorescent-BTx staining) and muscle fibre diameter (toluidine blue staining) in wild-type, *Ln* and Ca_v2.1-KO diaphragm muscle. N=5 mice per genotype, 10-20 NMJs/fibres measured per muscle. *p<0.05, †p<0.01, ‡p<0.001, different from wild-type, percentage change indicated in parentheses.

Discussion

We characterized the basic properties of ACh release and the compensatory contributions of non-Ca_v2.1 channels at NMJs of the natural *Cacna1a* mutant mouse *Ln*, and compared it with Ca_v2.1-KO NMJs. Despite similar neurological symptoms (severe ataxia and epilepsy) and a similar basic NMJ functional phenotype (~50% reduced ACh release, compared to

wild-type), a completely different compensatory profile of non- $Ca_v2.1$ channel contribution was revealed between the two mutants. This is the first report showing the consequences of the *Ln Cacna1a* mutation on neurotransmitter release *directly* measured at a single synapse. The reduction of ACh release at the *Ln* NMJ and the compensatory Ca_v channel profile are discussed below.

Reduced nerve stimulation-evoked neurotransmitter release at the Ln NMJ

The *Ln* phenotype is caused by a splice site mutation, giving rise to two novel $Ca_v2.1$ *Cacna1a* transcripts ('long' and 'short') with truncated cytoplasmic C-terminals (Fletcher et al., 1996; Doyle et al., 1997). Although histology indicated normal mRNA and $Ca_v2.1 \alpha_1$ protein level in the *Ln* cerebellum (Lau et al., 1998), electrophysiological studies showed reduced Ca^{2+} current density (Lorenzon et al., 1998; Dove et al., 1998; Wakamori et al., 1998). This implicates functional abnormalities of the *Ln*-mutated $Ca_v2.1$ channel. Indeed, ~70% reduced open-probability and a small positive shift of activation- and inactivation voltage were shown (Dove et al., 1998; Wakamori et al., 1998). Thus, our observation of ~50% reduced quantal content at the *Ln* NMJ can be explained by reduced presynaptic Ca^{2+} influx during a nerve action potential, following from impaired function of individual *Ln*-mutated $Ca_v2.1$ channels. It is unclear whether reduced $Ca_v2.1$ channel *number* also contributes. The compensatory involvement of $Ca_v2.3$ channels suggests that this may indeed be the case (see below).

Besides a lower initial ACh release, *Ln* NMJs showed a more pronounced EPP amplitude rundown than wild-type NMJs during 40 Hz repetitive stimulation. Normal rundown at wild-type NMJs (by about ~23%) is likely determined by multiple factors: $Ca_v2.1$ channel inactivation, its recovery, and replenishment of releasable transmitter vesicles. Rundown normally becomes less pronounced (or even reverses in run-up) at low quantal content, e.g. upon partial inhibition of $Ca_v2.1$ channels with submaximal concentrations of ω -agatoxin-IVA (S. Kaja, unpublished observation) or reduction of channels by anti- $Ca_v2.1$ antibodies (Lambert and Elmqvist, 1971). The less pronounced rundown in these cases most likely results from the Ca^{2+} influx level being within a critical range (not saturating the Ca^{2+} sensor of the release mechanism), in combination with accumulation of cytoplasmic Ca^{2+} during the repetitive stimulation. Our observation of *more* EPP rundown at the *Ln* NMJ, despite lowered quantal content, therefore indicates that *Ln*- $Ca_v2.1$ channels possess abnormal biophysical properties, rather than just being reduced in number. Although it is as yet unclear how the larger coefficient of variance of *Ln* EPP amplitude during 40 Hz trains is caused, this effect points to altered channel characteristics rather than to impaired replenishment of synaptic vesicles for release. Like at *Ln* NMJs, we found ~50% reduction of quantal content at NMJs from $Ca_v2.1$ -KO mice, compared to wild-type, confirming the findings in an earlier generated other $Ca_v2.1$ -KO mouse (Urbano et al., 2003).

We observed a reduced (~40-50%) muscle fibre diameter at *Ln* and $Ca_v2.1$ -KO diaphragms, compared to wild-type, most likely resulting from growth retardation (*Ln* and $Ca_v2.1$ -KO body weight was ~55% lower than wild-type). In normal muscle, fibre diameter is known to be inversely related with electrical input resistance, which, in turn, dictates MEPP amplitude (Katz and Thesleff, 1957). Furthermore, fibre diameter is positively correlated with NMJ size and ACh release level (Harris and Ribchester, 1979; Plomp et al., 1992). Therefore, the reduced muscle fibre diameter may explain the somewhat increased MEPP amplitude, compared to wild-type, measured at *Ln* and $Ca_v2.1$ -KO NMJs. In agreement with the smaller fibre diameter, we observed ~30% reduced NMJ area at *Ln* and $Ca_v2.1$ -KO NMJs, compared to wild-type. Hence, some of the reduction of ACh release may result from smaller motor nerve terminals.

An about 50% reduced nerve stimulation-evoked ACh release, accompanied by reduced synapse size, has also been shown at NMJs in muscle biopsies from two EA2 patients heterozygous for *CACNA1A* mutations leading to a severely truncated and non-functional $\text{Ca}_v2.1$ protein (Jen et al., 2001; Maselli et al., 2003a). Compensatory contribution of $\text{Ca}_v2.2$, but not Ca_v1 channels, was found. The similarities between EA2 and *Ln* and/or $\text{Ca}_v2.1$ -KO NMJs suggest that these mice might serve as a model for human EA2, as hypothesized earlier on the basis of CNS studies in these mice (for review, see Pietrobon, 2005b).

Spontaneous ACh release is reduced at Ln NMJs

Spontaneous unquantal ACh release at the wild-type mouse NMJ is for a large part dependent on $\text{Ca}_v2.1$ channels, as demonstrated by the 50-75% inhibition of MEPP frequency by 200 nM ω -agatoxin-IVA (this study; Plomp et al., 2000; Giovannini et al., 2002; Van Den Maagdenberg et al., 2004). We previously hypothesized opening of normal $\text{Ca}_v2.1$ channels already at resting membrane potential (Plomp et al., 2000). The ~50% reduced MEPP frequency at *Ln* NMJs, compared to wild-type, indicates reduced presynaptic Ca^{2+} influx at the resting motor nerve terminal, presumably due to impaired *Ln*- $\text{Ca}_v2.1$ channel function, as elaborated above. The observed ~50% reduction of MEPP frequency at $\text{Ca}_v2.1$ -KO NMJs confirms the reduction reported in the $\text{Ca}_v2.1$ -KO mouse generated by Urbano et al. (2003). About 40% of the spontaneous ACh release at $\text{Ca}_v2.1$ -KO NMJs is mediated by $\text{Ca}_v2.3$ channels, as indicated by the SNX-482 experiments. The insensitivity of MEPP frequency to ω -conotoxin-GVIA and nifedipine, in contrast to the sensitivity of evoked ACh release (see above), indicates that the Ca^{2+} influx at resting potential through Ca_v1 and $\text{Ca}_v2.2$ channels is too small to trigger release. This may be explained by these channels being localized more distantly from release sites than $\text{Ca}_v2.3$ channels (Urbano et al., 2003), or opening less at resting membrane potential.

Differential compensatory contribution of non- $\text{Ca}_v2.1$ channels at Ln and $\text{Ca}_v2.1$ -KO NMJs

Despite the phenotypic and NMJ function similarities between *Ln* and $\text{Ca}_v2.1$ -KO mice, we found an intriguingly distinct profile of compensatory contribution of non- $\text{Ca}_v2.1$ channel to evoked ACh release: at *Ln* NMJs there was ~10% contribution of $\text{Ca}_v2.3$ channels and ~25% of an unidentifiable Ca_v channel, while at $\text{Ca}_v2.1$ -KO NMJs there was contribution of Ca_v1 (~20%), $\text{Ca}_v2.2$ (~25%) and $\text{Ca}_v2.3$ (~50%) channels. Apparently, compensatory expression of these channel types is less needed at the *Ln* NMJ. These different profiles allow for some speculation on the mechanisms underlying recruitment of compensatory Ca_v channels. Our data suggest that the remaining *Ln*- $\text{Ca}_v2.1$ channels preclude compensatory contribution of $\text{Ca}_v2.2$ channels completely, and that of $\text{Ca}_v2.3$ channels partly. It has been hypothesized that transmitter release sites have type-specific 'slots' that are preferentially filled with $\text{Ca}_v2.1$ channels, but in their absence become occupied by $\text{Ca}_v2.3$ channels (Urbano et al., 2003; Cao et al., 2004). Since *Ln*- $\text{Ca}_v2.1$ channels still contribute to ACh release, the carboxy-terminal tail is apparently not absolutely required for 'slot' occupation, despite harbouring an active zone interaction site (Maximov et al., 1999). Carboxy-terminal redundancy in subcellular $\text{Ca}_v2.1$ localization has also been suggested in recent expression studies (Hu et al., 2005). The cytoplasmic synaptic protein interaction (synprint) site, remaining intact in *Ln*- $\text{Ca}_v2.1$ channels, may be of importance. It binds exocytotic machinery components (for review, see Spafford and Zamponi, 2003), and may thereby allow (*Ln*-) $\text{Ca}_v2.1$ channels to localize at active zones. Although $\text{Ca}_v2.2$ channels possess a synprint site, they apparently do not occupy 'slots' at *Ln* as well as wild-type NMJs. Possibly, $\text{Ca}_v2.2$ channels are inhibited through $\text{Ca}_v2.1$ channel-mediated Ca^{2+} influx stimulating syntaxin1A expression (Sutton et al., 1999),

subsequently promoting G-protein-dependent inhibition of $Ca_v2.2$ channels (Jarvis et al., 2000). Such a mechanism may also explain compensatory recruitment of $Ca_v2.2$ channels at the $Ca_v2.1$ -KO NMJ. However, $Ca_v2.3$ channels do not have a synprint site but are compensatorily contributing to ACh release at *Ln* as well as $Ca_v2.1$ -KO NMJs. Thus, there must be other mechanisms as well. For instance, the β_4 accessory subunit can affect channel recruitment by combined binding to multiple sites on the Ca_v2 subunit, including one at the C-terminus (Cornet et al., 2002). Such binding uninhibits a $Ca_v2.1$ protein retention signal to the endoplasmic reticulum exerted by the I-II loop (Bichet et al., 2000; Cornet et al., 2002). Since the C-terminal is absent in *Ln*- $Ca_v2.1$ protein, reduced β_4 -binding may cause some retention of $Ca_v2.1$ subunits and in this way allow $Ca_v2.3$ channel incorporation.

About 25% of the evoked ACh release at *Ln* NMJs was insensitive to compounds blocking either Ca_v1 , $Ca_v2.1$, $Ca_v2.2$ or $Ca_v2.3$ channels. Possibly, this remainder derives from Ca^{2+} influx through SNX-482 insensitive $Ca_v2.3$ channel isoforms (Tottene et al., 2000; Wilson et al., 2000; Sochivko et al., 2002) or through Ca_v3 (T-type) channels, although the latter channel is less likely because it lacks synaptic interaction sites and has not yet been associated with neurotransmitter release (Catterall, 2000).

Our finding of compensatory Ca_v1 involvement in evoked ACh release at NMJs of $Ca_v2.1$ -KO mice contrasts the study of Urbano et al (2003), where no such contribution was identified using 10 μ M nimodipine, despite immunohistochemical demonstration of $Ca_v1.3$ (α_{1D}) channel presence (Pagani et al., 2004). Subtle genetic background differences between our two $Ca_v2.1$ -KO mouse lines may be one factor accounting for this differential profile. Furthermore, although age of experimental mice was not explicitly noted in the paper of Urbano and colleagues (Urbano et al., 2003), lower quantal content and MEPP frequency, larger MEPP amplitude and smaller NMJ size of their wild-type mice, compared to wild-type values in the present study, suggest that experimental groups were younger than the ~20 days of age at which we performed experiments. The possibility cannot be excluded that compensatory Ca_v1 contribution only first develops during the third postnatal week.

Some cross-activity on non- $Ca_v2.3$ channels has been reported for SNX-482, although the emerging picture is very inconsistent (Newcomb et al., 1998; Neelands et al., 2000; Bourinet et al., 2001; Arroyo et al., 2003). If true, some degree of distortion might be present in our Ca_v subtype-characterizations. However, the reducing effect of 1 μ M SNX-482 on quantal content at $Ca_v2.1$ -KO NMJs after treatment with 2.5 μ M ω -conotoxin-IVA is similar to the effect of SNX-482 alone (S. Kaja, unpublished data). This excludes $Ca_v2.2$ channel block by SNX-482 at the mouse NMJ. Most studies characterizing SNX-482 specificity showed a lack of effect of the toxin on Ca_v1 channels, and we assume this also holds for the NMJ. Only Bourinet et al. (2001) described incomplete and reversible block of transfected Ca_v1 channels by 1.5 μ M SNX-482. Several studies demonstrated that SNX-482 (up to 1 μ M) had no effect on $Ca_v2.1$ channels (Newcomb et al., 1998; Urbano et al., 2003; Kaja et al., 2006; this study). It is surprising, therefore, that Arroyo et al. (2003) suggested efficient block of $Ca_v2.1$ channels by 0.3 μ M SNX-482.

Further insights into the exact mechanism of compensatory expression of Ca_v channels at synapses will be instrumental in understanding the cell type-specific effects of *Cacna1a* mutations.

